

IGNEOUS INTRUSION MODELS FOR FLOOR FRACTURING IN LUNAR CRATERS. R.W. Wichman and P.H. Schultz, Dept. of Geological Sciences, Brown University, Providence, RI 02912.

INTRODUCTION: Lunar floor-fractured craters are primarily located near the maria (1,2,3) and frequently contain ponded mare units and dark mantling deposits (3,4,5). Fracturing is confined to the crater interior, often producing a moat-like feature near the floor edge, and crater depth is commonly reduced by uplift of the crater floor (3). Although viscous relaxation of crater topography can produce such uplift (6,7,8), the close association of modification with surface volcanism supports a model linking floor fracture to crater-centered igneous intrusions (3,4,5). A previous study (3) proposed several intrusion models on the basis of observed crater morphology and elevation data. In this study, we quantitatively explore the consequences of two intrusion models for the lunar interior. The first model is based on terrestrial laccoliths and describes a shallow intrusion beneath the crater. The second model is based on cone sheet complexes where surface deformation results from a deeper magma chamber. In this abstract, we describe both models, their fit to observed crater modifications and possible implications for local volcanism.

THE LACCOLITH MODEL: Laccoliths are nearly circular, tabular to domical intrusions that develop from an initial sill-like form by the uplift of overlying strata (9,10,11). Deformation is concentrated along the periphery of the intrusion in the form of either a monoclinial fold or an arcuate, near-vertical fault, depending on the ductility of the country rock (11,12). In certain cases, peripheral dikes extend upward and away from the laccolith edge (12). The nature of deformation changes with time, since failure around the intrusion modifies the interaction of the intrusion with the confining medium. For the initial sill, deformation is localized by stress concentrations at the edge of the intrusion and depends on P_d , the difference between total magma pressure and local lithostatic pressure (10). As the sill grows, the net upward load on the overburden increases in proportion to the floor area and eventually exceeds the rigid strength of the crust (9,11). If the overlying section flexes as a layered sequence of elastic plates, the extent of uplift is related to the size of the intrusion, the driving pressure, P_d , and the effective elastic thickness of the overburden, T_e (12). Later, after failure separates the uplifted block from its surroundings, this block is totally supported by the intrusion. The magma column in the laccolith balances the driving pressure in the feeder dike and intrusion thickness is directly related to P_d (12).

Deformation over a laccolith can account for many aspects of floor fracturing. The uplift of strata above a laccolith resembles the observed uplift of crater floors. Ring faulting near the edge of a laccolith can yield the observed moat structures and associated volcanic vents. Extension of peripheral concentric dikes from the intrusion could explain the degradation and concentric graben observed outside the crater rim in the most extreme cases of lunar floor fracture (3). The relation between driving pressure and lithostatic pressure, however, may confine most deformation to crater interiors: increased lithostatic pressure beneath a topographic rise reduces P_d and should diminish uplift of the crater rim. Finally, the range of modified crater forms on the Moon is consistent with the derived sequence of deformation. The least modified floor-fractured craters, showing little uplift and no moat features, may represent simple flexure with minor peripheral faulting, whereas the apparent magmatic equilibration of floor elevations in more modified craters (3) would result from late stage magmatic support of the roof block.

From the model, floor fracturing can provide information about the lunar interior. First, since elastic deformation does not thin the roof block, uplift provides an estimate for intrusion thickness. Consequently, if the uplifted floor diameter delineates the laccolith size, floor uplift reflects the magmatic driving pressure and the effective elastic thickness. Since T_e describes flexure of the floor plate as a single elastic layer, it represents the minimum possible depth to the intrusion. The uplifted section, however, probably does not deform as a single elastic layer and the true stratigraphic thickness for a layered sequence can be as much as $\sim 6T_e$ (12), a maximum estimate for intrusion depth. Driving pressure represents the magmatic overpressure in an intrusion and is related to the magma column length beneath that intrusion (10). Since mare basalt magmas appear to be denser than the lunar crust, near-surface magmas on the Moon require a magma source at depth in the mantle (13); this mantle depth can be estimated from P_d if the crustal thickness and magma density are known.

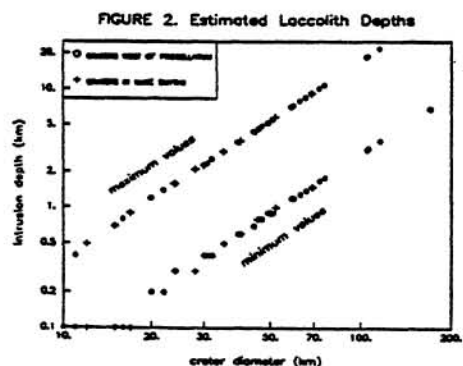
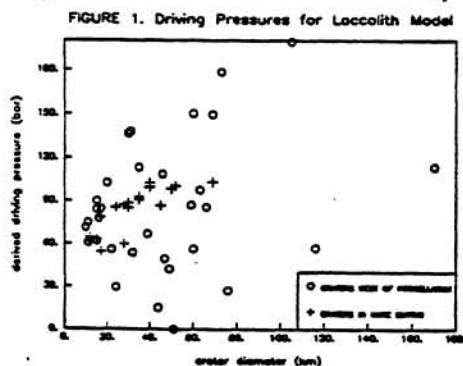
These relations have been applied to floor-fractured craters in Mare Smythii and west of Oceanus Procellarum (figure). The uniform driving pressures in Smythii are consistent with a common magma source of regional extent beneath the old impact basin. In contrast, the driving pressures west of Procellarum are widely scattered, with the lowest pressures corresponding to points adjacent to or isolated from clusters of floor-fractured craters. Since confined viscous flow causes a lateral pressure drop along a conduit (10), the distribution west of Procellarum could reflect the localization of subsurface magmas to a few areas revealed by extensive crater modification. The derived range of intrusion depths for both regions (figure) is consistent with both the emplacement depths of terrestrial laccoliths (~ 3 – 4 km, 14) and hydrostatic models of mare magma columns (magma depths less than 4 – 6 km, 13). The larger crater diameters west of Procellarum, however, require slightly deeper intrusions since T_e is also a function of intrusion size. Hydrostatic magma columns rise higher if the mantle is shallow; hence, the regional differences in both intrusion depth and P_d may mirror

mantle topography. The uniformly shallow magmas in Smythii lie over a broad (~360 km dia), uniform mantle uplift at the center of the impact basin. West of Procellarum, however, the crust is thicker and no single basin dominates mantle topography. Instead, floor fracturing clusters near individual large craters (70–170 km dia) which may have perturbed the upper mantle.

Terrestrial laccoliths differ from the observed crater modifications in two ways. First, laccoliths on Earth rarely exceed 10 km in diameter, whereas the modeled diameters for floor fracturing range from ~10 km to over 60 km. This discrepancy, however, may reflect the broadly fractured nature of impact breccias and weaker confining pressures due to the lower lunar gravity. Second, coherent uplift of the crater floor as a whole contrasts with the uniform size of terrestrial laccoliths. Once terrestrial laccoliths have sufficient leverage to lift overburden, vertical growth occurs at the expense of lateral expansion (12). Since lunar rocks are colder and drier than terrestrial rocks, they should be less ductile; hence ring faulting should develop soon after uplift begins and also prevent further lateral growth. The observed floor uplift/crater rim diameter ratios, however, indicates that uplift on the Moon occurs only when intrusions approach the size of the crater floor. Nevertheless, such behavior might be expected if lateral expansion of a sill is unhindered beneath the crater floor but confining pressures under the crater rim, due to either the edge of brecciation or surface topography, force vertical rather than horizontal growth.

THE CONE SHEET MODEL: On Earth, cone sheet complexes are composed of inwardly-dipping, sub-parallel dikes exposed in a circular or elliptical plan typically 10–20 km in diameter (15,16). Individual sheets are only 3–15 m thick, but they usually form a belt 1–3 km wide around a central region with few intrusions (16). Anderson estimated the uplift across one such complex to be ~1100 m (16). While local stratigraphy controls laccolithic intrusions, cone sheets result from magma injected into axially symmetric fractures induced by dilation of a central magma chamber at depth (15,16,17). The depth and the small size of the magma chamber make the resulting fractures relatively insensitive to surface topography (15). Since cone sheet geometry is nearly invariant, the only real parameter that can be derived from this model is the depth of the source intrusion. If the edge of the floor plate marks the surface trace of the innermost cone sheets, then these sheets probably dip down to the source at between 45° and 70° (16).

The combined offsets across a swarm of cone sheets can produce the required floor uplifts for lunar floor-fractured craters. The concentration of deformation into an annulus surrounding a relatively coherent central block also resembles the concentration of fracture in moats around the crater floor plate, with cone sheets feeding the floor volcanism that preferentially occurs near the floor edge (3). The mean floor diameter west of Procellarum (~36 km) indicates magma chamber depths of ~18–50 km, while mean intrusion depths are ~10–21 km in Smythii. The maximum depths are on the order of the estimated crustal thicknesses (18) for both regions, whereas shallower intrusion depths (derived for the smallest craters) might reflect intrusions tapping major cone sheets centered on a deeper source intrusion beneath adjacent, larger craters.



Two difficulties, however, limit modeling floor fracture by cone sheet emplacement. First, strong radial components commonly associated with cone sheet formation (17,19) are typically absent from lunar patterns of floor fracture (3). Second, cone sheet deformation centered on a crater is difficult to envision. On Earth, impact fractures and slump faults do not reach depths comparable to the floor radius (20,21) and the depth of brecciation is similarly shallow (20). Since the derived source intrusion depths on the Moon exceed the floor block radius, there is no clear-cut structural control to center the cone sheet source beneath a crater. Although the derived depths may be consistent with a source at the base of the crust, only the largest crater-forming impacts could disturb the crust-mantle boundary and create a mantle uplift or trap for subsequent magma accumulation. Deep central intrusions, however, may not be necessary; rather, shallower intrusions may reactivate the slump faults, thereby producing cone sheet-like dikes beneath the crater rim. In particular, this might occur near laccolithic intrusions, since the peripheral dikes surrounding a laccolith should intercept these faults at depth.

REFERENCES: 1) Brennan, W.J. (1975) *Moon* 12, 449–461. 2) Whitford-Stark, J.L. (1974) *Nature* 248, 573–575. 3) Schultz, P.H. (1976) *Moon* 13, 241–273. 4) Young, R.A. (1972) *Apollon 16 Prelim. Sci. Rep.*, NASA SP-315, 29–69 + 29–90. 5) Bryan, W.B. et al (1975) *LPSC* 6, 2563–2570. 6) Dancz, Z.F. (1965) *Astronom. Stud. Ann. Prog. Rep. A* (1964–1965), 81–100. 7) Scott, R.F. (1967) *Icarus* 7, 139–148. 8) Hall, J.L. et al (1981) *J. Geophys. Res.* 86, 9337–9352. 9) Gilbert, G.K. (1877) *Report on the Geology of the Henry Mountains*. 10) Johnson, A.M. and Pollard, D.P. (1973) *Tectonophysics* 18, 261–309. 11) Corry, C.E. (1988) *Geol. Soc. Amer. SP-220*. 12) Pollard, D.P. and Johnson, A.M. (1973) *Tectonophysics* 18, 261–309. 13) Solomon, S.C. (1975) *LPSC* 6, 1021–1042. 14) Jackson, M.D. and Pollard, D.P. (1983) *Geol. Soc. Amer. Bull.* 100, 117–139. 15) Anderson, E.M. (1956) *Proc. Roy. Soc. Edin.* 56, 128–157. 16) Phillips, W.J. (1974) *Tectonophysics* 24, 69–84. 17) Koide, H. and Bhattachary, S. (1975) *Econ. Geol.* 70, 781–799. 18) Bratt, S.R. et al (1985) *J. Geophys. Res.* 90, 3049–3064. 19) Komaru, H. (1987) *J. Volcan. Geotherm. Res.* 31, 139–149. 20) Pohl, J. et al (1977) *Impact and Explosion Cratering*, pp. 343–404. 21) Scott, D. and Hajnal, Z. (1988) *Meteoritics* 23, 239–248.